

Energy Transfer in Spherical Geometry

Application to Micelles

Mário N. Berberan-Santos and Manuel J. E. Prieto*

Centro de Química Estrutural, Complexo I, Instituto Superior Técnico, Av. Rovisco Pais, 1096 Lisboa Codex, Portugal

A model for long-range dipole-dipole energy transfer in spherical geometry is presented which, from steady-state or time-resolved fluorescence measurements, enables the determination of the relative positions of donor and acceptor inside the sphere. Its application to micelles (sodium dodecyl sulphate, SDS, and Triton X-100) did not lead to a quantitative determination of the position of the probes [*n*-(9-anthroyloxy) stearic acids, *n*-AS, (*n* = 2, 3, 6, 9, 12) and functional rhodamine and cyanine dyes], and this fact is attributed to probe-induced perturbations on the micellar structure. The results obtained lead to the following conclusions: (i) functional probes in micelles have specific radial positions and (ii) the perturbed region is a preferential solubilization site for a second probe.

Singlet-singlet energy transfer is well described by a dipole-dipole interaction¹ (Förster's very weak coupling limit²), with its characteristic r^{-6} dependence, if the donor-acceptor distance is not very small ($r > ca. 5 \text{ \AA}^3$). This explicit distance dependence has allowed its application for probing structural details of molecular assemblies namely reversed micelles⁴ and normal micelles.⁵⁻¹⁹

The assessment of probe location in the micelle by techniques other than energy transfer, namely n.m.r.,^{20,21} fluorescence (spectral shifts, lifetimes and quenching)²²⁻²⁴ and absorption,^{25,26} gave ample evidence of preferential positions in the micelle, but mainly on a qualitative basis. A quantitative study by energy transport has been reported.²⁷ Probe location by energy transport is, however, severely hampered by the requirement of fluorescent molecules with appropriate Förster radius for homotransfer.

The purpose of the present paper is the derivation of a model for energy transfer in spherical geometry and its application in the determination of probe location in micelles. This model encompasses previous treatments, where donor and acceptor are assumed to be on the same spherical surface²⁸ or where one of the molecules is located at the centre of the sphere.¹⁴

The Model

Donors and acceptors are distributed by spheres according to the Poisson law.²⁹ Sphere-sphere interactions are neglected.

We assume a specific radial location; in the general case this is different for donor and acceptor and varies from the centre to the surface of the sphere. In this way, two concentric spherical surfaces with radii R_s and a are defined (fig. 1). The radial parameter a defines the position of the inner partner, while the position of the outer partner is described by the parameter R_s .

The usual assumptions for the dipolar mechanism are assumed, *i.e.* point dipoles in isotropic and fast rotation (dynamic regime³⁰) at a fixed distance. Therefore the model is static, except for the rotational motion of the partners. Energy transport, *i.e.* donor-donor transfer, is also not considered (this implies in general no more than one donor

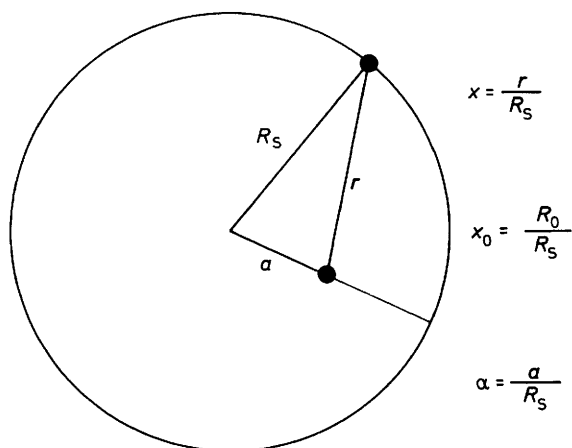


Fig. 1. Geometry and parameters of the system.

per sphere or large Stokes shift for the donor molecule), neither are back-transfer and non-linear effects.

The mathematical treatment is simplified by considering the following adimensional parameters: adimensional relative distance $x = r/R_s$, adimensional radial parameter $\alpha = a/R_s$, adimensional Förster radius $x_0 = R_0/R_s$ and adimensional time $\theta = t/\tau$, where τ is the donor's lifetime in the absence of energy transfer.

The distance distribution function for the donor-acceptor pair is³¹

$$f(x) = x/2\alpha \quad x \in [1-\alpha, 1+\alpha]. \quad (1)$$

Considering a population of spheres with n acceptor molecules at distances r_1, r_2, \dots, r_n from the donor, and assuming linearity, the equation that describes the time evolution of D^* , following a $\delta(t)$ -type excitation, is

$$dD^*/dt = \delta(t) - 1/\tau D^* - \sum_{i=1}^n (1/\tau)(R_0/r_i)^6 D^* \quad (2)$$

whose solution is

$$\rho_n(\theta, x_0, \dots, x_n) = \prod_{i=0}^n \exp[-(x_0/x_i)^6 \theta] \quad (3)$$

where ρ is the probability of finding the donor molecule excited at time θ .

Introducing the distance distribution function (1), the decay becomes

$$\rho_n(\theta, \alpha, x_0) = \int_{1-\alpha}^{1+\alpha} \int_{1-\alpha}^{1+\alpha} \dots \int_{1-\alpha}^{1+\alpha} \prod_{i=0}^n x_i/2\alpha \exp[-(x_0/x_i)^6 \theta] dx_0 dx_1 \dots dx_n \quad (4)$$

and can be rewritten as

$$\rho_n = J^n \exp(-\theta) \quad (5)$$

where

$$J = J(\theta, \alpha, x_0) = \int_{1-\alpha}^{1+\alpha} x/2\alpha \exp[-(x_0/x)^6 \theta] dx. \quad (6)$$

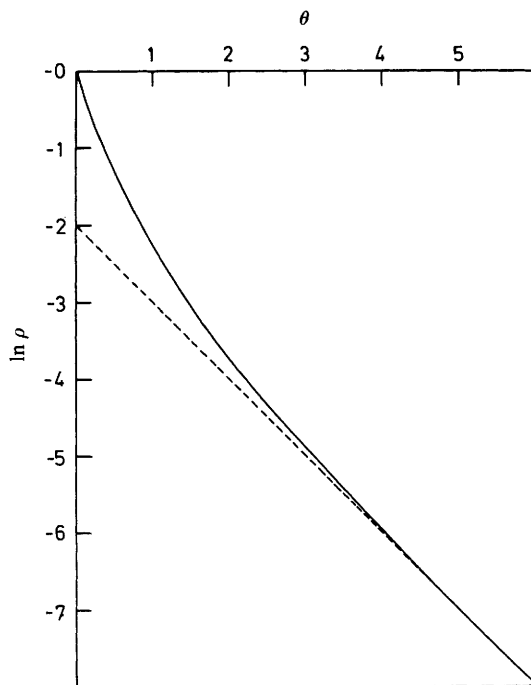


Fig. 2. Donor decay curve [eqn (8)] for $\alpha = 0$, $x_0 = 1$, $\mu = 2$ (—); asymptotic decay (---). The intercept and slope of the straight line are μ and 1, respectively.

Taking into account the Poissonian distribution of acceptors with a mean occupation number μ ($\mu = [\text{acceptor}]/[\text{sphere}]$), the macroscopic decay is expressed as

$$\rho(\theta, \alpha, x_0, \mu) = \sum_{n=0}^{\infty} \rho_n \mu^n \exp(-\mu)/n! \quad (7)$$

or

$$\rho = \exp(-\theta) \exp[-\mu(1-J)]. \quad (8)$$

A simulated decay curve is shown in fig. 2. Asymptotic behaviour towards an exponential decay is observed, as at large times only donors in spheres with no acceptors are still decaying.

Eqn (8), which describes the donor's decay when excited by a $\delta(t)$ pulse, can be formulated as

$$dD^*/dt = \delta(t) - k_D D^* - k(t) D^* \quad (9)$$

where $k_D = 1/\tau$, and $k(t)$ is the time-dependent rate constant for energy transfer obtained from eqn (8).³²

$$k(t) = -\mu \partial J / \partial t. \quad (10)$$

The acceptor molecule is then excited by a pulse whose profile is $k(t) D^*$.

Returning to the analysis of the donor kinetics, the expression for the photostationary state is obtained by integration of eqn (8)

$$\phi / \phi_0 = \int_0^{\infty} \exp(-\theta) \exp[-\mu(1-J)] d\theta \quad (11)$$

where ϕ and ϕ_0 are the donor's quantum yields in the presence and absence of acceptor.

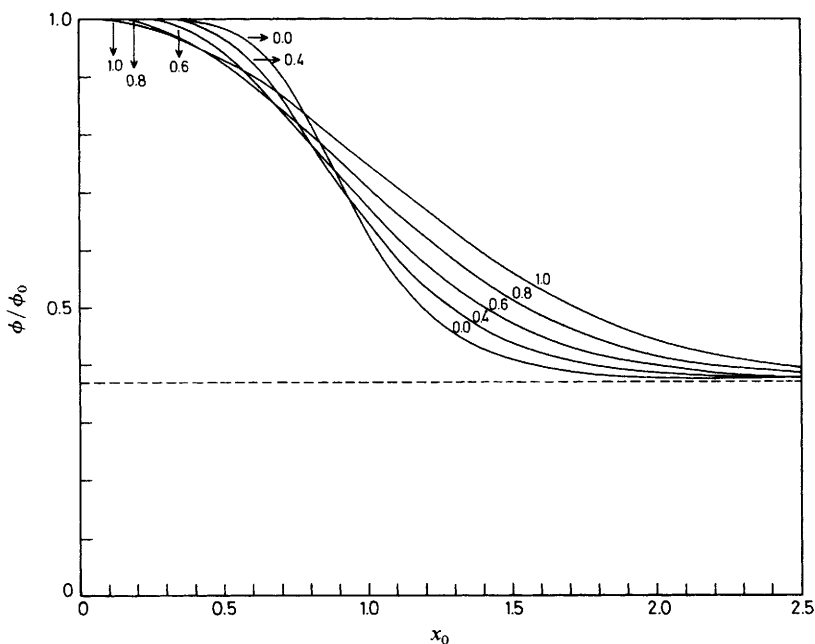


Fig. 3. Plot of ϕ/ϕ_0 vs. x_0 [eqn (11)] with $\mu = 1$ for different values of the radial parameter α (—). The asymptote [$\exp(-1)$, Perrin's limit] is also shown (---)

Eqn (11) can also be written as

$$\phi/\phi_0 = \sum_{n=0}^{\infty} \mu^n [\exp(-\mu)/n!] \phi_n/\phi_0 \quad (12)$$

where

$$\phi_n/\phi_0 = \int_0^{\infty} J^n \exp(-\theta) d\theta \quad (13)$$

i.e. the relative quantum yield of spheres with n acceptor molecules [eqn (13)], has analytical solution for some particular cases (Appendix 1).

In fig. 3 the result of the calculation of ϕ/ϕ_0 vs. x_0 [eqn (11)] is shown for several values of α , when the mean occupation number of acceptor is $\mu = 1$.

A crossing region is apparent in fig. 3. While for low values of x_0 , fluorescence quenching is greater when donor and acceptor are both on the sphere surface ($\alpha = 1$), the opposite happens for higher values of x_0 , when the energy transfer process is more efficient if one of the probes is located at the sphere's centre ($\alpha = 0$). This is easily understood on the grounds of an active sphere surrounding the donor and considering the possible donor-acceptor distances for each α .

For large x_0 ($R_0 \gg R_s$), the Perrin limit³³ [$\exp(-\mu)$] is attained, and when x_0 is small ($R_0 \ll R_s$) the above equations reduce to the well known formulae for energy transfer in a planar geometry^{34,35} (Appendix 2).

Note that previous treatments by Marszalek *et al.*¹⁴ ($\alpha = 0$), Sato and coworkers^{18,19} and Eisinger *et al.*²⁸ ($\alpha = 1$), are contained as particular cases in the present model.

In the above derivation we have assumed the usual approximation of fast and isotropic rotation of the dipoles (dynamic regime). A treatment considering the intermediate regime, where energy transfer and molecular rotations have the same timescale,

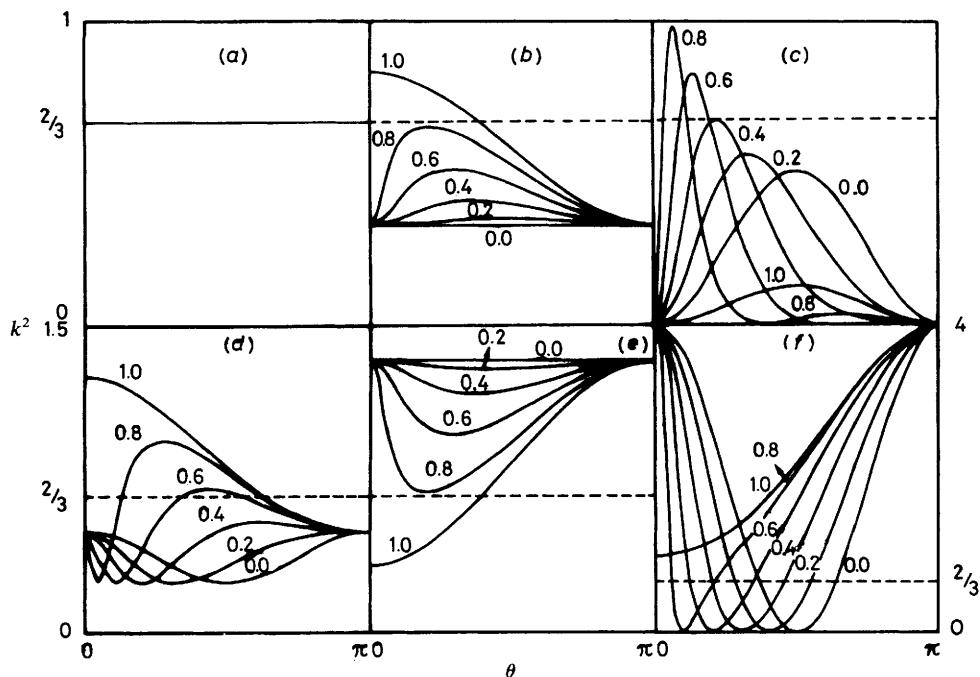


Fig. 4. Orientational factor k^2 vs. angular distance θ for various values of the radial parameter α ; the dipoles are either radial (L), planar (P) or isotropic (I). (a) I-I, (b) P-I, (c) L-P, (d) P-P, (e) L-I, (f) L-L.

has been carried out,³⁶ but it suffices here to discuss limiting situations; the latter will be invoked in the interpretation of the experimental results.

When there is complete absence of molecular rotation, and the dipoles are randomly distributed with regard to both distance and orientation, the appropriate value of the orientational factor is $k^2 = 0.476$.³⁰ Therefore, it cannot, in general, be used with other distributions of distances.

Taking into account an average over orientations,³⁷ J [eqn (6)] is given by

$$J = \int_{1-\alpha}^{1+\alpha} x/2\alpha \int_0^1 \int_0^1 \exp\{-\theta(x_0/x)^6[3/2(3y^2+1)z^2]\} dy dz dx. \quad (14)$$

The absence of dipolar rotations, as assumed in the static limit, must imply a lower energy-transfer efficiency, which is confirmed by calculation [eqn (14)].

The dipolar anisotropic distribution deserves detailed treatment. Following Eisinger *et al.*,²⁸ three possible orientations of the dipoles are considered: radial (L), planar (P) and isotropic (I). The orientational factor k^2 is then calculated performing appropriate averages. The result, a function of θ , angular separation and α , the radial parameter, is shown in fig. 4 for the six possible cases.

From these plots it can be anticipated that, in general, the efficiency of transfer will be lower than in the isotropic case. This is confirmed by the calculation of the relative quantum yield ϕ/ϕ_0 . It must be stressed that the evaluation of molecular distances *via* the dipolar mechanism is not so critically dependent on the orientational factor as could be expected. As Haas *et al.*³⁸ pointed out, single-dipole transitions and/or completely frozen rotations are limiting situations seldom verified.

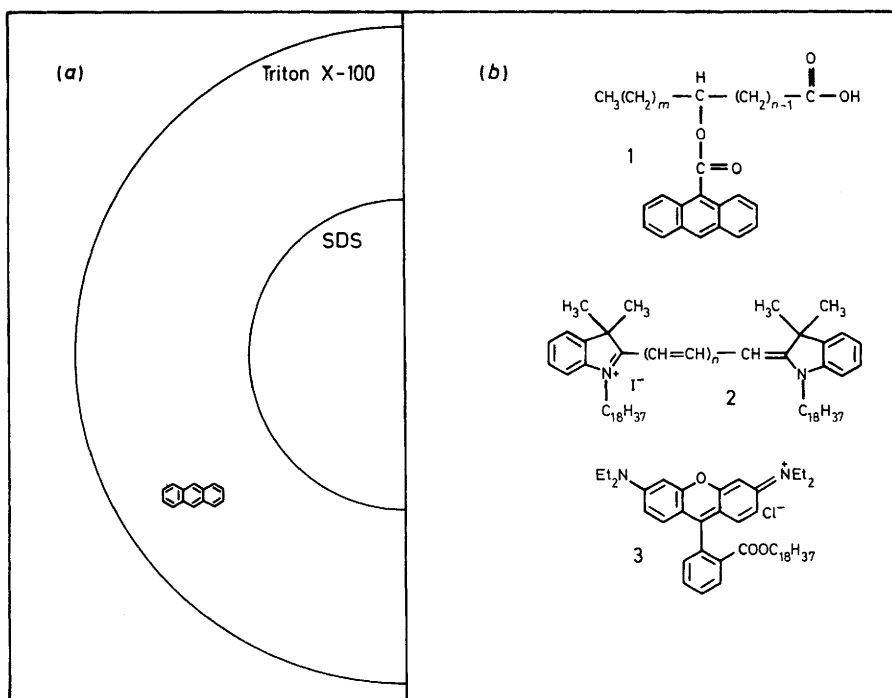


Fig. 5. (a) Schematic representation of relative dimensions of the surfactant micelles Triton X-100 and SDS, and of the anthracene moiety. (b) Molecular structures of (1) *n*-AS, (2) di-I-C₁₈-(2n + 1), (3) ORB.

Experimental

Materials

The functional probes, *n*-(9-anthroyloxy) stearic acids (*n*-AS; *n* = 2, 3, 6, 9, 12), the cyanines 1,1'-dioctadecyl-3,3,3',3'-tetramethylindocarbocyanine iodide [di-I-C₁₈-(3)] and 1,1'-dioctadecyl-3,3,3',3'-tetramethylindodicarbocyanine iodide [di-I-C₁₈-(5)], and octadecyl rhodamine B chloride (ORB), were obtained from Molecular Probes (Eugene, Oregon) and are shown in fig. 5(b).

The surfactants, Triton X-100 (BDH, scintillation grade) and sodium dodecylsulphate (SDS, Merck, p.a.), were used as received. Methyl anthroate was synthesised by standard procedures and 9,10-diphenylanthracene (DPA) was from Koch-Light (scintillation grade).

Methods

Triton X-100 micellar solutions were prepared in phosphate buffer (pH 7.4) of low ionic strength, while for SDS a 0.1 mol dm⁻³ NaCl solution was used to lower the c.m.c.,³⁹ and in this way suppress radiative energy transfer.

n-AS was dissolved by adding an ether solution (<1 cm³) to a hot (45 °C) and well stirred micellar solution, these conditions being maintained until complete evaporation of the ether. Identical results were obtained *via* direct probe solubilization.

Low micellar concentrations were used (10^{-4} mol dm $^{-3}$) and the solutions were allowed to stand for two days before measurements.

The solutions were not degassed. Oxygen quenching in micelles is not expected to be relevant at atmospheric conditions except for molecules with long lifetimes.⁴⁰ The observed decrease in quantum yield due to the presence of oxygen was always <5%.

Fluorescence spectra were obtained at 25 °C using a Perkin-Elmer MPF-3 spectrofluorimeter equipped with a thermostating unit. 5 × 5 mm cells were used. Excitation and emission bandwidths were 4 nm. Radiative transfer was negligible in the described experimental conditions.

For the calculation of R_0 , emission spectra were corrected using a calibration curve obtained from fluorescence standards.⁴¹ The absorption spectra were recorded on a Perkin-Elmer Lambda 5 spectrophotometer.

Fluorescence decays were measured using the time-correlated single-photon counting technique. The excitation source was a nitrogen-filled flash lamp (Edinburgh Instruments, 199 F). Alternated collection of pulse and sample profiles, detected with a Philips XP2020Q photomultiplier, was performed. The decay curves were deconvoluted on a Digital PDP 11/23 computer, employing the method of modulating functions.⁴²

Data fitting and numerical integrations were carried out on a Digital Equipment Corp. VAX 11/780 computer.

Results and Discussion

The selected micellar systems were Triton X-100 (non-ionic, micellar radius = 43 Å,⁴³ aggregation number $\nu = 140$ –150⁴³) and SDS (anionic, hydrophobic radius = 20 Å, calculated⁴⁴ with an aggregation number $\nu = 91$ in 0.1 mol dm $^{-3}$ NaCl⁴⁵), as these two micelles are well described in the literature and have different physical characteristics, namely size.

For the family of *n*-AS probes there is evidence that anthroate chromophores are located at a graded series of depths from the surface, depending on their substitution positions in the aliphatic chain.^{23,46–49} In addition, these probes have moderate-to-short lifetimes, depending on the environment, which implies negligible lateral diffusion when used as donors in energy-transfer experiments in micelles.

The other partner of the Förster pair was chosen according to the following requirements: (i) complete absence in the aqueous 'phase', *i.e.* strict micellar solubility, (ii) no inner filter effect of the acceptor at the excitation wavelength, (iii) $R_0 \approx R_s$, this being a very important condition [In fact, if energy transfer is very efficient ($x_0 \gg 1$), no information about the probe location can be assessed from a steady-state study, as in this case total fluorescence quenching is obtained in micelles containing one or more acceptor molecules (Perrin's active sphere³³). This situation is reached for $R_0 > 2.5 R_s$, as is apparent from fig. 3. In transient-state studies this limit is actually somewhat higher, its value depending on the time resolution. Kasatani *et al.* were successful at $x_0 = 2.7$.¹⁹], (iv) known location, as this would provide a test of the results.

Functional cyanine and rhodamine probes were selected as acceptors for the *n*-AS probes, and DPA was also used as donor.

In SDS micelles, Triton X-100 (monomer) was used as donor (phenoxy chromophore), the *n*-AS molecules acting in that case as acceptors. In this way the following systems were studied.

Triton X-100 Micelles

(1) *n*-AS ($n = 3, 6, 9, 12$), DPA, donors and ORB, acceptor. (2) *n*-AS ($n = 2, 12$), donor, and di-I-C₁₈-(3), acceptor. Spectra of these probes are shown in fig. 6 and the quantum yields ϕ_0 of the donors are reported in table 1. The R_0 values, reported in table 2, were

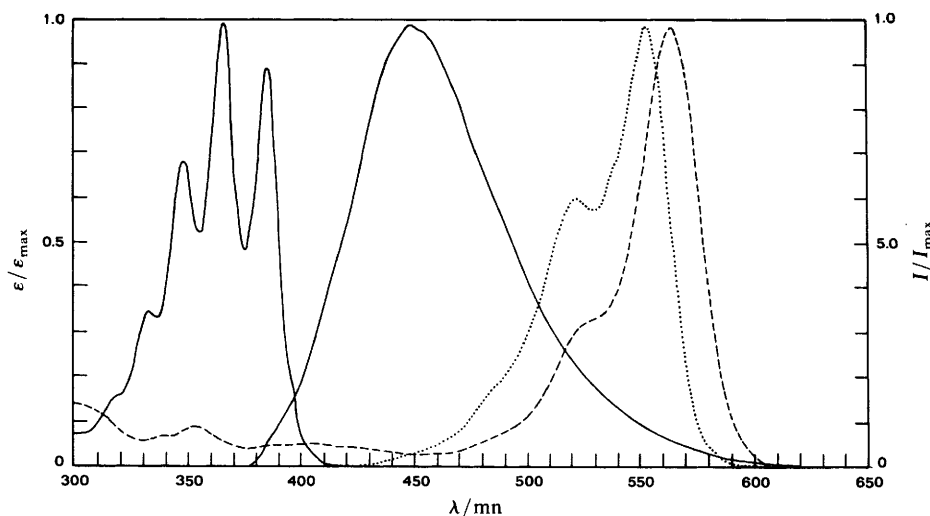


Fig. 6. Absorption and fluorescence spectra in Triton X-100 micelles of the probes: 12-AS [(—) $\epsilon(365 \text{ nm}) = 6.2 \times 10^3 \text{ dm}^3 \text{ mol}^{-1} \text{ cm}^{-1}$; $\lambda_{\text{ex}} = 385 \text{ nm}$], di-I-C₁₈-(3) [(···) $\epsilon(552 \text{ nm}) = 1.2 \times 10^5 \text{ dm}^3 \text{ mol}^{-1} \text{ cm}^{-1}$], ORB [(---), $\epsilon(563 \text{ nm}) = 7.4 \times 10^4 \text{ dm}^3 \text{ mol}^{-1} \text{ cm}^{-1}$].

Table 1. Fluorescence quantum yields ϕ_0 of the probes in micelles of Triton X-100 and SDS (aerated solutions)

probe	micelle	
	Triton X-100	SDS
DPA	1.0 ^a	—
2-AS	0.14 ^b	0.07 ^b
3-AS	0.18 ^c	0.07 ^c
6-AS	0.31 ^b	0.08 ^b
9-AS	0.41 ^b	0.12 ^b
12-AS	0.55 ^b	0.15 ^b
Triton X-100	0.32 ^d	0.30 ^e

^a Determined *vs.* DPA in cyclohexane, $\phi_F = 0.90$.⁵⁰ ^b Ref. (46); variation <5% in the presence of O₂. ^c Interpolated value. ^d Ref. (9). ^e Determined *vs.* naphthalene in cyclohexane, $\phi_F = 0.23$.⁵¹

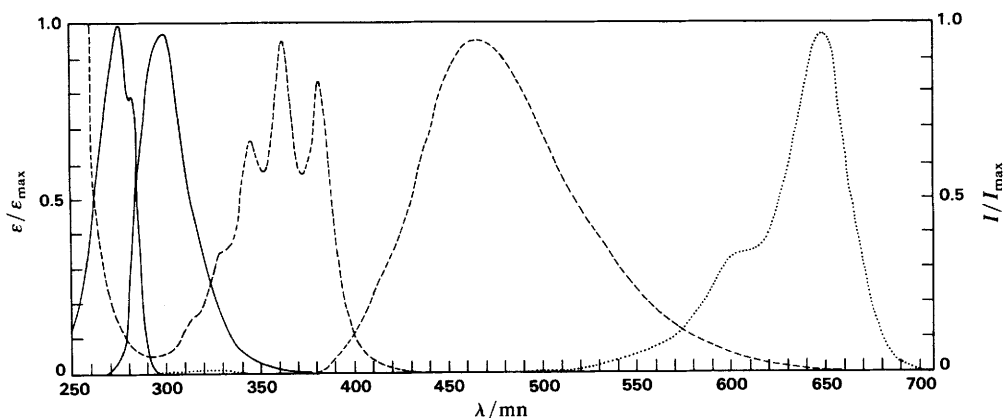
calculated from Förster's formula, rewritten as

$$R_0 = 0.2108 \left(k^2 \phi_0 n^{-4} \int_0^\infty I(\lambda) \epsilon(\lambda) \lambda^4 d\lambda \right)^{1/6} \quad (15)$$

with R_0 in Å, where k^2 is the orientational factor, ϕ_0 is the donor quantum yield in the absence of acceptor, n is the refractive index of the medium, $I(\lambda)$ is the normalized fluorescence spectrum, $\epsilon(\lambda)$ is the molar extinction coefficient ($\text{dm}^3 \text{ mol}^{-1} \text{ cm}^{-1}$) and λ is in nm.

Table 2. Förster critical radius R_0 (Å) [eqn (15) with $k^2 = 2/3$ and $n = 1.33$] for the donor-acceptor pairs solubilized in Triton X-100 and SDS micelles

acceptor	donor	R_0/A
Triton X-100		
di-I-C ₁₈ -(3)	2-AS	46
di-I-C ₁₈ -(3)	12-AS	53
di-I-C ₁₈ -(3)	DPA	37
ORB	3-AS	38
ORB	6-AS	42
ORB	9-AS	43
ORB	12-AS	45
SDS		
di-I-C ₁₈ -(5)	3-AS	31
di-I-C ₁₈ -(5)	12-AS	29
3-AS	Triton X-100	19
12-AS	Triton X-100	19

**Fig. 7.** Absorption and fluorescence spectra in SDS micelles of the probes: Triton X-100 (monomer) [(—) $\epsilon(280 \text{ nm}) = 1.4 \times 10^3 \text{ dm}^3 \text{ mol}^{-1} \text{ cm}^{-1}$; $\lambda_{\text{ex}} = 280 \text{ nm}$]; 3-AS [(- - -) $\epsilon(365 \text{ nm}) = 6.8 \times 10^3 \text{ dm}^3 \text{ mol}^{-1} \text{ cm}^{-1}$; $\lambda_{\text{ex}} = 385 \text{ nm}$]; di-I-C₁₈-(5) [(· · ·) $\epsilon(649 \text{ nm}) = 1.8 \times 10^5 \text{ dm}^3 \text{ mol}^{-1} \text{ cm}^{-1}$].

SDS Micelles

(1) n -AS ($n = 3, 12$), donors and di-I-C₁₈-(5), acceptor. (2) Triton X-100 (monomer), donor, and n -AS ($n = 3, 12$), acceptor. Spectra of the probes are presented in fig. 7, and the ϕ_0 and R_0 values are reported in tables 1 and 2.

The energy-transfer study was carried out by measuring the donor's fluorescence intensity as a function of μ , the mean number of acceptors per micelle. Micellar concentrations were calculated with c.m.c. values of $2.4 \times 10^{-4} \text{ mol dm}^{-3}$ for Triton X-100⁵² and $1.6 \times 10^{-3} \text{ mol dm}^{-3}$ for SDS in 0.1 mol dm^{-3} NaCl.³⁹

Results for the system n -AS, ($n = 3, 12$) DPA/ORB in Triton X-100 are presented in fig. 8. Similar data are obtained for 6-AS and 9-AS, which are omitted for simplicity. From these results it is apparent that the energy-transfer efficiency varies in the sequence $\text{DPA} < 3\text{-AS} < 6\text{-AS} < 9\text{-AS} < 12\text{-AS}$. However, if it is taken into account that R_0 values have the same trend (table 2) no immediate conclusion can be derived about the relative radial position of these probes.

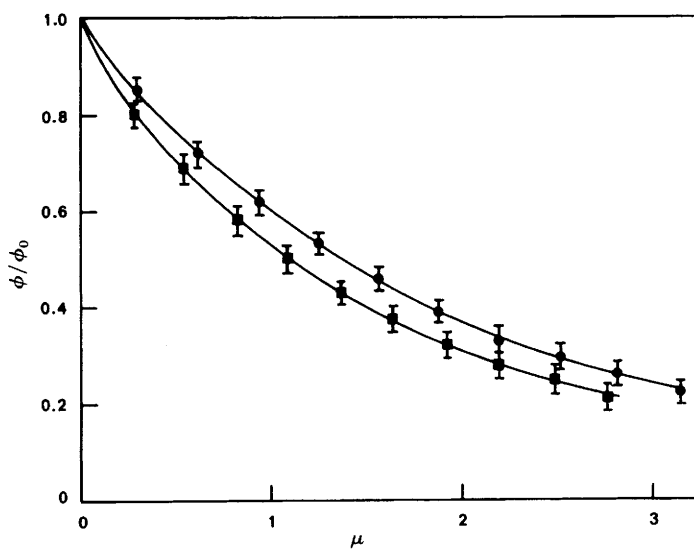


Fig. 8. Relative quantum yields of fluorescence ϕ/ϕ_0 , for the probes 3-AS (●) and 12-AS (■) vs. μ (ORB) in Triton X-100 micelles.

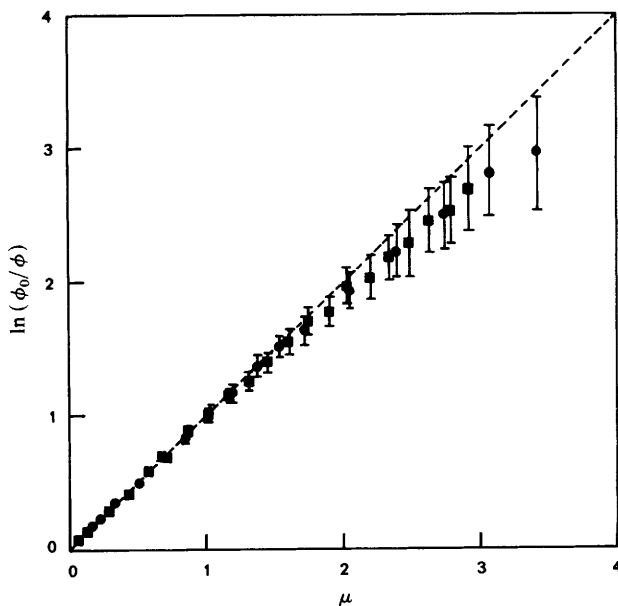


Fig. 9. Plot of $\ln(\phi_0/\phi)$ for the 2-AS (●) and 12-AS (■) probes vs. μ [di-I-C₁₈-(3)] in Triton X-100 micelles.

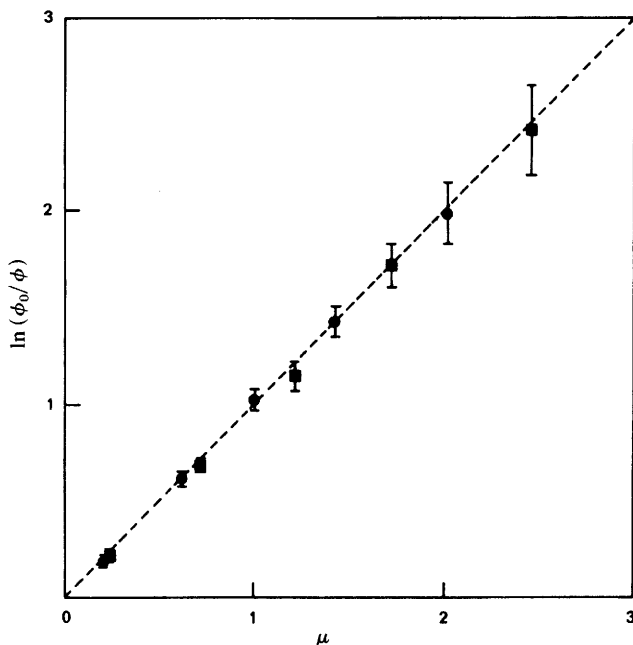


Fig. 10. Plot of $\ln(\phi_0/\phi)$ for the 3-AS (●) and 12-AS (■) probes vs. μ [di-I-C₁₈-(5)] in SDS micelles.

The results for the system n -AS-di-I-C₁₈-(3) in Triton X-100 (fig. 9) show a very high efficiency of energy transfer. A logarithmic plot is used to show that for $\mu < 2$ the donor's quenching is complete in micelles with at least one acceptor (Perrin mechanism).

The occurrence of such an efficient process is not readily understood on the basis of the expected x_0 values for this system. However, two relevant conclusions can be drawn: (i) a Poisson distribution is obeyed at least up to $\mu = 2$ and (ii) the mean occupancy number, μ , was correctly calculated.

One of the systems in SDS micelles, n -AS-di-I-C₁₈-(5), gave similar results (fig. 10) and the above considerations and conclusions are also applicable to it. For the Förster pairs, Triton X-100 (monomer)- n -AS ($n = 3, 12$), in SDS micelles, different quenching efficiencies were again obtained for the two n -AS probes, as can be seen in fig. 11. As in this case R_0 is the same for both pairs (table 2), the results imply different radial positions for 3- and 12-AS, and this is thought to be the first time this conclusion has been obtained from energy-transfer studies.

Application of the Model

The pair of parameters (x_0, α) can in principle be obtained from a fit to the experimental curve (ϕ/ϕ_0 vs. μ), i.e. it is theoretically possible to obtain the absolute locations of donor and acceptor from steady-state studies. Owing to the complex dependence in eqn (11), a linear least-squares fit is not possible. Thus, a direct point-to-point calculation of the 'goodness-of-fit' S^2 was made:

$$S^2(x_0, \alpha) = \sum_i [y_i(\text{exptl}) - y_i(\text{calc.})]^2 \quad (16)$$

where $y_i = \phi/\phi_0(\mu_i)$. The S^2 mapping yields a smooth surface crossed by a 'canyon' where the minimum values are located, a typical result being represented in fig. 12(a) for the system 12-AS/ORB in Triton X-100 micelles. The search for the best (x_0, α)

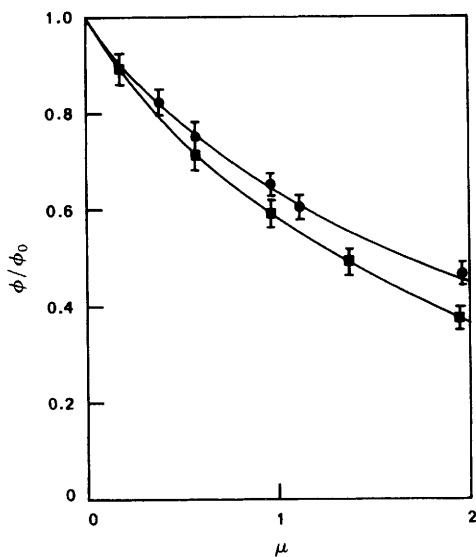


Fig. 11. Relative yields of fluorescence, ϕ/ϕ_0 , of Triton X-100 (monomer) vs. μ [3-AS (●) and 12-AS (■)] in SDS micelles.

pair was performed by moving along the canyon's bed, looking for its deepest point [fig. 12(b)].

For 12-AS/ORB (Triton X-100 micelles), while a well defined minimum was not obtained, it seems possible to conclude that the 12-AS probe occupies an internal position inside the sphere with $\alpha < 0.3$, i.e. no more than 11 Å off-centre, if R_s (the location of the ORB probe) is assumed to be 37 Å.²⁷ However, systematic application of this fitting procedure led to unacceptable results; for some systems the minimum values were not at all defined, while for other they were unreasonable or showed no logical sequence.

In order to understand these results, theoretical curves were produced for the extreme radial situations, and it was verified that both reproduced the observed curves within experimental error. In this way a steady-state experiment will usually only enable one to recover precisely the curve $x_0 = x_0(\alpha)$ [see fig. 12(a)], i.e. a collection of correlated (x_0, α) pairs but not the best one. This fact arises from steady-state-limited accuracy and also from the restricted range of μ values (say $0 < \mu < 2$), but not from any theoretical restriction of the model, as previously inferred.¹⁹

In order to rationalize the results we have used plots similar to fig. 3. As in this case the only known experimental value is ϕ/ϕ_0 , a value for x_0 must be assumed for plotting the data.

This methodology was applied to the system DPA, *n*-AS-ORB (acceptor) in Triton X-100 micelles. The value of $R_s = 37 \pm 2$ Å reported for ORB²⁷ was used, assuming that in a Triton X-100 micelle of 43 Å radius⁴³ this probe is externally positioned with respect to the donor probes *n*-AS. This is reasonable, given the molecular structure of ORB, as the ionic chromophore should prefer a superficial position. Then, from the spectroscopic values of R_0 (table 2) the values of $x_0 = R_0/R_s$ depicted in fig. 13 ($\mu = 2$) were obtained.

It can be seen that no logical radial sequence is obtained for the set of probes and, in addition, DPA and 3-AS are even outside the range permitted by the model delimited by the curves $\alpha = 0$ and $\alpha = 1$. It should be stressed that the results are quite reproducible (for ϕ/ϕ_0 differences < 0.02 were obtained). The previously rejected hypothesis of having the DPA, *n*-AS externally located, i.e. that these probes would define the R_s ,

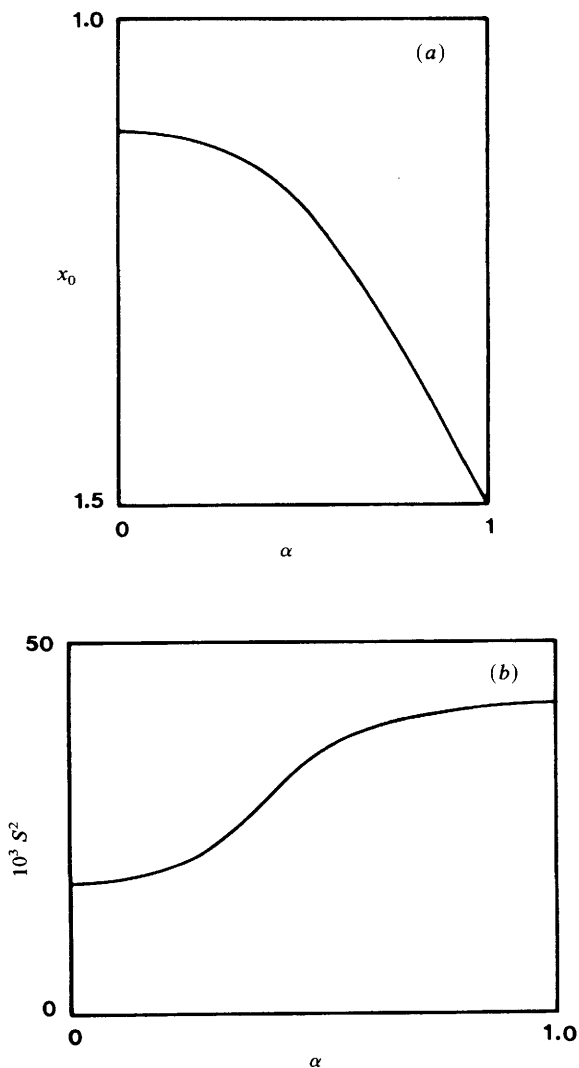


Fig. 12. (a) Plot of the 'canyon' of minimum values of the function S^2 [eqn (16)] on the surface (x_0, α) for the system 12-AS/ORB in Triton X-100 micelles. (b) Values of the function S^2 [eqn (16)] along the 'canyon' of minimum values on the surface (x_0, α) for the system 12-AS/ORB in Triton X-100 micelles.

value, would imply still lower x_0 values. Besides, any change to the reported value of 37 \AA for the ORB position would merely imply an abscissa translation of all the points and an unreasonable sequence of positions would again be obtained. The same trend of variation was obtained for other values of μ , so this behaviour cannot be specifically ascribed to high occupation numbers.

The application of identical methodology to the systems in SDS micelles is not possible since the R_s value is not known from previous studies, but a range for R_s can be estimated, corresponding to the limits of α ($\alpha = 0$ and $\alpha = 1$), so an evaluation of the micellar radius is accessible. The experimental values of $\phi/\phi_0 = 0.46$ [Triton X-100 (monomer)/3-AS (acceptor)] and $\phi/\phi_0 = 0.37$ [Triton X-100 (monomer)/12-AS (acceptor)], both for $\mu = 2$, define in fig. 13 (together with the curves of the model) a common

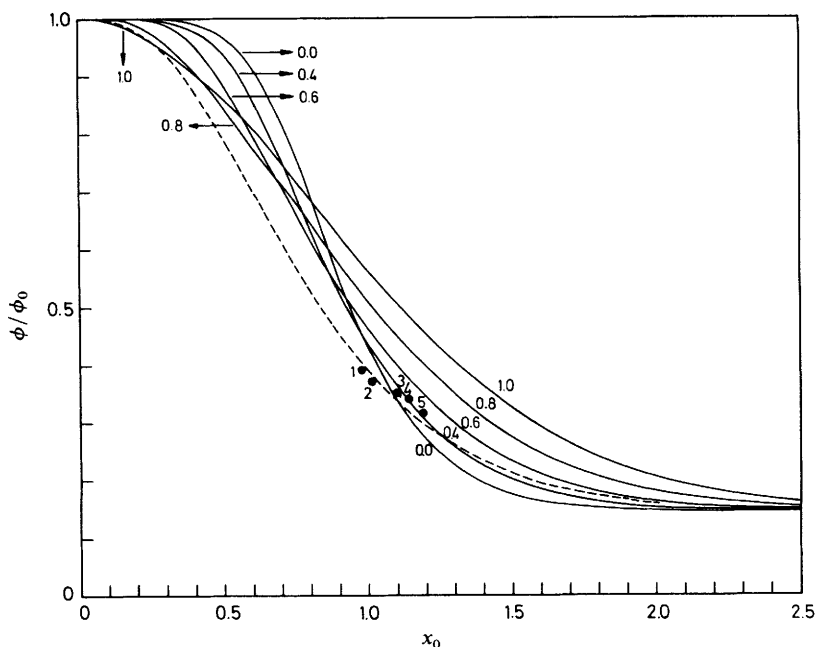


Fig. 13. Plot of ϕ/ϕ_0 vs. x_0 with $\mu = 2$ [eqn (11)] for several values of the radial parameter α (—), and assuming homogeneous distribution of probes in the micellar volume (---). Attributed values on the basis of $R_s = 37 \text{ \AA}$ for the systems: DPA(1), 3-AS(2), 6-AS(3), 9-AS(4), 12-AS(5)/ORB in Triton X-100 micelles.

region of x_0 values between 1.06 and 1.17, with α indeterminate. Assuming a common value of R_s [defined by the Triton X-100 (monomer) probe], a value of $R_s = 17\text{--}18 \text{ \AA}$ is obtained, in agreement with a reported superficial location of this chromophore in an SDS micelle.²⁵

The described difficulties with the adequateness of the model/experiment, namely the obtention of precise radial location, are even more severe for the systems involving the cyanines, both in Triton X-100 and SDS micelles. In fact, the existence of a mechanism of total quenching (Perrin) is not rationalizable given the R_0 values as previously reported, unless very small R_s values with no physical meaning are assumed.

Before proceeding into further reasoning, it is important to re-examine the assumptions of the model.

Geometry and Configuration of the Micellar System

Micellar Sphericity. The SDS micelle, in the presence of 0.1 mol dm^{-3} NaCl, is considered to be spherical.^{23,25} The Triton X-100 micelle is eventually ellipsoidal,⁴³ but the deviations due to this geometry would be minimal and an 'average radial position' should be obtained as reported by other authors.²⁷

Monodispersity. For both micelles the size distribution is quite narrow,⁵³ therefore this assumption is reasonable. Besides, were this effect important, it would imply deviation to the observed Poisson distribution.²⁹

Solute Distribution by Micelles. Although a Poisson distribution has been observed in a great number of cases,²⁹ it was suggested⁵⁴ that for very hydrophobic molecules such as the functional probes used, an alternative distribution could be obeyed. However, a

simple calculation shows that this distribution gives an even lower efficiency of energy transfer. In any case, this distribution must be rejected, as the systems in which the cyanines are involved verified the Perrin formulation with clear evidence of the Poisson distribution (the results in accordance with Dorrance-Hunter statistics⁵⁴ would be quite different).

Inter-micellar Energy Transfer. The micellar concentration never exceeded 10^{-4} mol dm^{-3} . For this concentration, the average micellar distance (140 Å) is much greater than the R_0 values and therefore this contribution can be neglected. Furthermore, translational diffusion of the micelles is unimportant during the donor's lifetime.

Radial Probe Location. The assumption of a well defined radial location is certainly an idealization and it is more reasonable to consider a probe distribution centred in an average position. In this case only small deviations to the model would occur and its application should even then allow the determination of the average radial position.

The other limit is a homogeneous distribution of probes within the micelle, whose distance distribution function is³¹

$$f(x) = 3x^2/16(x-2)^2(x+4) \quad (17)$$

previously obtained *via* a Monte-Carlo simulation.¹⁷

The result of its application in the context of the present model is shown in fig. 13 for $\mu = 2$. For the system DPA, *n*-AS/ORB (acceptor) in Triton X-100 micelles a generally good agreement is obtained, with only the 9-AS and 12-AS probes showing deviations from the theoretical curve. From the set of probes $R_s = 37\text{--}40$ Å is obtained.

However, a homogeneous distribution must be ruled out on the basis of the following arguments: (a) there is convincing evidence by independent methods of a variation of physical properties along the series of *n*-AS probes when solubilized in micelles, which implies distinct radial positions;^{23,46-49} (b) the observed Perrin formulation with the cyanine in the same Triton X-100 micelle would remain unexplained; (c) the previously described results for the system Triton X-100 (monomer)-*n*-AS shows that in SDS micelles the probes 3-AS and 12-AS have a different location.

After these considerations of the determination of solute location in micelles by energy transfer a critical comment on published studies^{8,14} would seem to be pertinent. In fact, it can be concluded that it is possible to obtain reasonable micellar radii with any distance distribution function (*i.e.* model) used ($\alpha = 0$, $\alpha = 1$ or even the homogeneous distribution). In this way it will be very difficult to infer anything about probe location in micelles when dealing with restricted models only supported by model-derived radii.

Restrictions to the Application of the Förster Formalism

Distance Distribution Function and Validity of the Dipolar Mechanism. Although near the limit $\alpha = 1$, the model assumes very short donor-acceptor distances, for which the dipolar approximation breaks down, the statistical weight of these cases is negligible. In addition, geometrical considerations based on molecular models evidentiate that excluded volume effects are unimportant [see *e.g.* fig. 5(a)] *i.e.* in this regard probes are independently distributed to a good approximation.

Orientalional Factor and Dipolar Mechanism. The observed anomalies on the model application must be analysed, taking into account the possible importance of the orientational factor.

In a first hypothesis the static isotropic limit described by eqn (14) can be considered. However, this situation would imply, in relation to the dynamic isotropic limit assumed in the model, a still lower efficiency of energy transfer, precisely the opposite of experimental evidence.

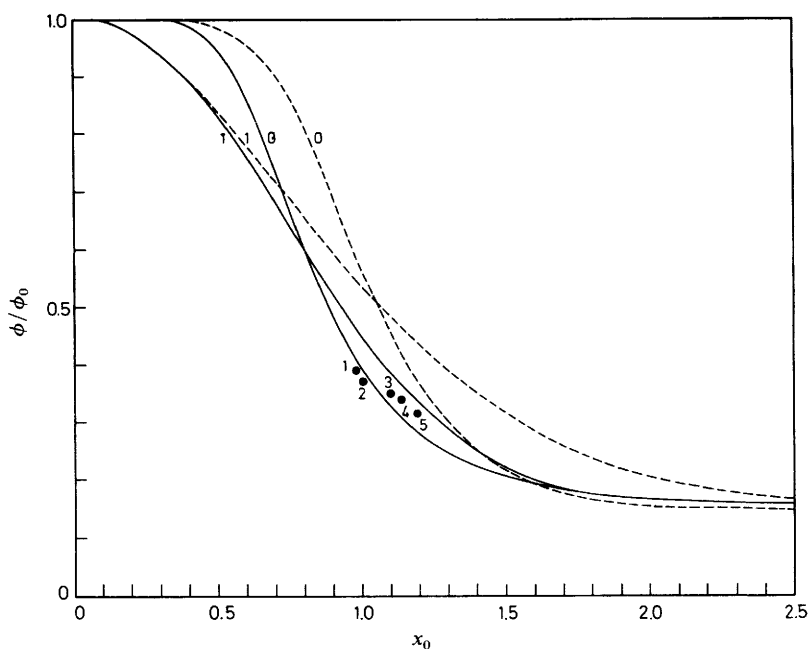


Fig. 14. Plot of ϕ/ϕ_0 vs. x_0 with $\mu = 2$ for the limit values $\alpha = 0$ and $\alpha = 1$, in situation of anisotropic energy transfer L-L (—) and P-P (---). Attributed values to the systems: DPA(1), 3-AS(2), 6-AS(3), 9-AS(4), 12-AS(5)/ORB in Triton X-100 micelles.

The dipolar anisotropy, on the other hand, could in principle justify some of the experimental results as the most favourable orientation ($k^2 = 4$) leads to a R_0 value 1.35 times greater than the one with $k^2 = 2/3$, although, as reported previously, this fact should not be overemphasized in energy-transfer studies. In addition, the fluorescence anisotropy observed for the n -AS probes is not very high ($r \approx 0.1$) and the distribution of dipoles over the spherical geometry would also attenuate the effect of any preferential orientation of the dipoles, as expected.

From the consideration of k^2 for the various anisotropic situations L, P, I (cf. fig. 4), the diagrams of ϕ/ϕ_0 vs. x_0 were obtained and the configurations L-L and P-P for the limits $\alpha = 0$ and $\alpha = 1$, when $\mu = 2$, are shown in fig. 14. It can be seen that the curves have the same trend as the ones for the I-I configuration, and there is no combination of L, P, I that globally explains the results.

Molecular Diffusion. This point deserves detailed attention, as the existence of significant diffusion would increase the energy-transfer efficiency.

Molecular diffusion in micelles is a complex problem owing to the inhomogeneous nature of the medium and also because the effective diffusion coefficient, D , is a function of radial location, so its value depends on the probe.

Recent results for the n -AS probes,⁴⁶ obtained from diffusion controlled fluorescence quenching studies, give for the diffusion coefficient of 2-AS probe in Triton X-100 micelles an upper bound of $1.25 \times 10^{-7} \text{ cm}^2 \text{ s}^{-1}$. Assuming for the other probe, e.g. ORB, an identical value, and considering that $\tau(2\text{-AS}) = 8.7 \text{ ns}$, the static approximation is shown to be valid as $\sqrt{(2D\tau)} \approx 7 \text{ \AA} \ll R_0$. The other donor used, Triton X-100 (monomer), also has a short lifetime, $\tau = 6.3 \text{ ns}$ in SDS.

Other evidence favouring the unimportance of molecular diffusion was obtained from an independent photophysical experiment. An n -AS chromophore analogue,

methyl anthroate, in homogeneous medium (dioxane) efficiently quenches ORB fluorescence (Stern-Volmer constant $K_{sv} = 14.7 \text{ dm}^3 \text{ mol}^{-1}$). For ORB in dioxane a lifetime $\tau = 1.8 \text{ ns}$ was measured, so the value for the quenching rate constant is $k_q = 8.1 \times 10^9 \text{ dm}^3 \text{ mol}^{-1} \text{ s}^{-1}$. Assuming the proper molecular radii,⁵⁵ geometrical factors⁵⁶ and transient effects a value for the diffusion-controlled rate constant $k_q = 8.6 \times 10^9 \text{ dm}^3 \text{ mol}^{-1} \text{ s}^{-1}$ is obtained, close to the experimental one. [A charge-transfer interaction is eventually involved, as the reduction potential of rhodamine B in the excited state is $E(\text{RhB}^*/\text{RhB}^{-*}) = +1.34 \text{ eV (vs. SCE)}$ ⁵⁷ and methyl anthroate will have as an upper bound to its ionization potential the value of anthracene 7.43 eV ,⁵⁸ so the charge-transfer process should be at most slightly endothermic].

In contrast with the previous experiment, it was not possible to quench the ORB fluorescence with 3-AS in Triton X-100 micelles, even for high values of the mean occupation number ($\mu = 10$). This fact demonstrates that isotropic diffusion is not important in these systems.

After reviewing the critical assumptions of the model and finding no apparent flaws in it is possible to invoke an explanation for the greater efficiency of energy transfer observed, when compared with the model prediction. Micellar perturbation induced by the probes seems to be a reasonable one.

The solubilization of a probe causes a local perturbation in the micellar structure, and the perturbed region is a preferential solubilization site for the second probe. In this way there is a population of donor-acceptor pairs at shorter distances than those assumed *i.e.* the model fails owing to the assumption of an independent distribution for the two molecules of the Förster pair. This hypothesis is further supported by the observed trends of variation: (i) functional probes with two hydrophobic tails (cyanines), induce greater perturbation (Perrin type fluorescence quenching) than probes with one tail [ORB, *n*-AS, Triton X-100 (monomer)]; (ii) probes with a more eccentric radial localization (DPA and 3-AS), induce greater perturbation relative to a surface adsorbed probe (ORB), on account of its vicinity.

It should be emphasized that the existence of this common region of solubilization does not imply the existence of molecular aggregates. Even for very low occupation numbers of acceptor ($\mu < 0.5$) the structural perturbations must be invoked, and in this case there is no significant micellar multi-occupation.

In this way, in the donor-acceptor containing micelles there exists no ground-state complex, as is also evident from the monomer absorption of these dyes. In addition, the existence of donor-acceptor aggregates would have been revealed by the fluorescence quenching of ORB, as in this case a static mechanism would be operative.

Therefore, our results seem to favour micelles as entities with a high structural organization. Evidence for similar structural perturbation has been reported recently.^{59,60} Time-resolved fluorescence studies and relaxation time measurements $T_1(^1\text{H})$, are in progress, to characterize further the reported facts.

Conclusions

A model for long-range dipole-dipole energy transfer in spherical geometry is presented which, from fluorescence intensity or decay measurements, enables the determination of the absolute positions of donor and acceptor inside the sphere.

Its steady-state application to micelles did not lead to a quantitative determination of the probe position and this fact was attributed to probe-induced perturbations on the micellar structure.

The results obtained lead to the following conclusions: (i) functional probes in micelles have specific radial positions, namely in SDS micelles the probe 12-AS has an inner location relative to the 3-AS probe; (ii) the probes perturb the micellar structure, giving rise to changes in their local environment in such a way that the perturbed region

is a preferential solubilization site for a second probe. The extent of perturbation apparently depends on the number of hydrophobic tails of the functional probe and on the donor-acceptor radial vicinity.

The present model, taking into account distinct radial positions, can be applied to obtain structural information in other spherical molecular assembly. The adimensional parametrization used, enables a quick evaluation of the potentialities of a specific Förster pair for the study of a given assembly.

This work was supported by Instituto Nacional de Investigação Científica (project 4/D). Time correlated single-photon counting instrumentation is acknowledged to the Alexander von Humboldt Foundation (F.R.G.). G. Striker is also gratefully acknowledged for the deconvolution program.

Appendix 1

Relative Quantum Yield of the Donor in a Sphere with n Acceptors

From eqn (6) and (13) we have

$$\phi_n/\phi_0 = \int_{1-\alpha}^{1+\alpha} \int_{1-\alpha}^{1+\alpha} \cdots \int_{1-\alpha}^{1+\alpha} \prod_{k=0}^n (x_k/2\alpha) / \sum_{k=0}^n (x_0/x_k)^6 dx_0 dx_1 \dots dx_n \quad (\text{A1a})$$

and for $\alpha = 0$

$$\phi_n/\phi_0 = 1/(1+nx_0^6). \quad (\text{A1b})$$

For $\alpha \neq 0$, only $n = 1$ has an exact solution

$$\begin{aligned} \phi_1/\phi_0 = & 1 + x_0^2/12\alpha (\ln \{[(a^2 - a + 1)/(b^2 - b + 1)]^{1/2}(b + 1)/(a + 1)\} \\ & + \sqrt{3}\{\arctan [\sqrt{3}/(2a - 1)] - \arctan [\sqrt{3}/(2b - 1)] - \pi f\}) \end{aligned} \quad (\text{A1c})$$

where

$$\begin{aligned} a &= [(1 + \alpha)/x_0]^2 & b &= [(1 - \alpha)/x_0]^2 \\ f &= \begin{cases} 1 & \text{if } x_0 \in [\sqrt{2}(1 - \alpha), \sqrt{2}(1 + \alpha)], \\ 0 & \text{otherwise.} \end{cases} \end{aligned}$$

Appendix 2

Transition from Spherical to Planar Geometry

Eqn (8) can be rewritten as

$$\rho = \exp(-\theta) \exp \left[-\sigma \int_h^{R_s+a} 2\pi r \{1 - \exp[-\theta(R_0/r)^6]\} dr \right] \quad (\text{A2a})$$

where $\sigma = \mu/4\pi R_s^2$ is the average superficial concentration and $h = R_s - a$. The transition from the spherical to the planar geometry is obtained for $R_s \rightarrow \infty$, and in this case h is the interplanar distance.

For $h = 0$ (donors and acceptors in the same plane), and denoting by n_0 the number of acceptor molecules in an area πR_0^2 , $n_0 = \sigma \pi R_0^2$,

$$\rho = \exp(-\theta) \exp[-\Gamma(2/3)n_0\theta^{1/3}] \quad (\text{A2b})$$

which is the well known formular for energy transfer by a dipolar mechanism, in two dimensions.³⁵

For donors and acceptors in parallel planes at a distance h , when $h \gg R_0$,

$$\rho = \exp(-\theta) \exp[-n_0/2(R_0/h)^4\theta]. \quad (\text{A2c})$$

This expression is the well known Kuhn result⁶¹ and is accurate for $h > 1.7R_0$.³⁴

References

- 1 Th. Förster, *Ann. Phys.*, 1948, **2**, 55.
- 2 Th. Förster, in *Modern Quantum Chemistry, Part III B*, ed. O. Sinanoglu (Academic Press, New York, 1965), pp. 93-137.
- 3 J. Eisinger, B. Feuer and A. A. Lamola, *Biochemistry*, 1969, **8**, 3908.
- 4 M. A. J. Rodgers and H. D. Burrows, *Chem. Phys. Lett.*, 1979, **66**, 238.
- 5 F. W. J. Teale, *Nature (London)*, 1958, **181**, 415.
- 6 G. S. Singhal, E. Rabinowitch, J. Hevesi and V. Srinivasan, *Photochem. Photobiol.*, 1970, **11**, 531.
- 7 M. Almgren, *Photochem. Photobiol.*, 1972, **15**, 297.
- 8 G. A. Kenney-Wallace, J. H. Flint and S. C. Wallace, *Chem. Phys. Lett.*, 1975, **32**, 71.
- 9 K. Kalyanasundaram and J. K. Thomas, in *Micellisation, Solubilization and Microemulsions*, ed. K. L. Mittal (Plenum Press, New York, 1977), vol. 2, pp. 569-588.
- 10 N. Roessler and G. Von Büнау, *J. Photochem.*, 1978, **9**, 307.
- 11 Y. Usui and A. Gotou, *Photochem. Photobiol.*, 1979, **29**, 165.
- 12 Y. Kusumoto and H. Sato, *Chem. Phys. Lett.*, 1979, **68**, 13.
- 13 T. Matsuo, Y. Aso and K. Kano, *Ber. Bunsenges. Phys. Chem.*, 1980, **84**, 146.
- 14 T. Marszałek, A. Baczyński, W. Orzeszko and A. Rozploch, *Z. Naturforsch., Teil A*, 1980, **35**, 85.
- 15 H. Sato, Y. Kusumoto, N. Nakashima and K. Yoshihara, *Chem. Phys. Lett.*, 1980, **71**, 326.
- 16 H. Sato, M. Kawasaki and K. Kasatani, *J. Photochem.*, 1981, **17**, 243.
- 17 P. K. F. Koglin, D. J. Miller, J. Steinwandel and M. Hauser, *J. Phys. Chem.*, 1981, **85**, 2363.
- 18 H. Sato, M. Kawasaki and K. Kasatani, *J. Phys. Chem.*, 1983, **87**, 3759.
- 19 K. Kasatani, M. Kawasaki, H. Sato and N. Nakashima, *J. Phys. Chem.*, 1985, **89**, 542.
- 20 K. A. Zachariasse and B. Kozankiewicz, in *Surfactants in Solution*, ed. K. L. Mittal and B. Lindman (Plenum Press, New York, 1984), vol. 1, pp. 565.
- 21 K. N. Ganesh, P. Mitra and D. Balasubramanian, *J. Phys. Chem.*, 1982, **86**, 4291.
- 22 M. Grätzel and J. K. Thomas, in *Modern Fluorescence Spectroscopy*, ed. E. L. Wehry (Plenum Press, New York, 1976), vol. 2, pp. 169-216.
- 23 E. Blatt and W. H. Sawyer, *Biochim. Biophys. Acta*, 1985, **822**, 43.
- 24 M. Almgren and S. Swarup, *J. Phys. Chem.*, 1982, **86**, 4212.
- 25 J. R. Cardinal and P. Mukerjee, *J. Phys. Chem.*, 1978, **82**, 1614.
- 26 P. Mukerjee and J. R. Cardinal, *J. Phys. Chem.*, 1978, **82**, 1620.
- 27 M. D. Ediger, R. P. Domingue and M. D. Fayer, *J. Chem. Phys.*, 1984, **80**, 1246.
- 28 J. Eisinger, W. E. Blumberg and R. E. Dale, *Ann. N.Y. Acad. Sci.*, 1981, **366**, 155.
- 29 M. Almgren and J.-E. Löfroth, *J. Chem. Phys.*, 1982, **76**, 2734.
- 30 J. Eisinger and R. E. Dale, *J. Mol. Biol.*, 1974, **84**, 643.
- 31 M. Berberan-Santos, *Am. J. Phys.*, 1986, **54**, 1139.
- 32 Eqn (10) can also be derived according to the procedure of Pilling and Rice, M. J. Pilling and S. A. Rice, *J. Chem. Soc., Faraday Trans. 2*, 1976, **72**, 792.
- 33 A. Yekta, M. Aikawa and N. J. Turro, *Chem. Phys. Lett.*, 1979, **63**, 543.
- 34 N. Shaklai, J. Yguerabide and H. M. Ranney, *Biochemistry*, 1977, **16**, 5585.
- 35 D. E. Koppel, P. J. Fleming and P. Strittmatter, *Biochemistry*, 1979, **18**, 5450.
- 36 J. Knoester and J. E. Van Himbergen, *J. Chem. Phys.*, 1984, **81**, 4380.
- 37 I. Z. Steinberg, *J. Chem. Phys.*, 1968, **48**, 2411.
- 38 E. Haas, E. Katchalski-Katzir and I. Z. Steinberg, *Biochemistry*, 1978, **17**, 5064.
- 39 M. Corti and V. DeGiorgio, *Chem. Phys. Lett.*, 1978, **53**, 237.
- 40 N. J. Turro, M. Aikawa and A. Yekta, *Chem. Phys. Lett.*, 1979, **64**, 473.
- 41 W. H. Melhuish, *Appl. Opt.*, 1975, **14**, 26.
- 42 G. Striker, in *Deconvolution and Reconvolution of Analytical Signals*, ed. M. Bouchy (University Press, Nancy, 1982), pp. 329-354.
- 43 R. J. Robson and E. A. Dennis, *Acc. Chem. Res.*, 1983, **16**, 251.
- 44 M. Almgren and S. Swarup, *J. Colloid Interface Sci.*, 1983, **91**, 256.
- 45 J. Kratochvíl, *J. Colloid Interface Sci.*, 1980, **75**, 271.
- 46 E. C. C. Melo, *Ph.D. Thesis* (Technical University of Lisbon, 1986).
- 47 M. J. E. Prieto, J. Villalaín and J. C. Gómez-Fernandéz, in *Spectroscopy of Biological Molecules*, ed. M. Manfait, A. J. P. Alix and L. Bernard (Wiley, New York, 1985), pp. 296-298.

- 48 E. Blatt and K. P. Ghiggino, *J. Chem. Soc., Faraday Trans. 1*, 1981, **77**, 2551.
- 49 E. Blatt, K. P. Ghiggino and W. H. Sawyer, *Chem. Phys. Lett.*, 1985, **114**, 47
- 50 S. R. Meech and D. Phillips, *J. Photochem.*, 1983, **23**, 193.
- 51 I. B. Berlman, *Handbook of Fluorescence Spectra of Aromatic Molecules* (Academic Press, London, 1965), p. 330.
- 52 A. Ray and G. Némethy, *J. Am. Chem. Soc.*, 1971, **93**, 6787.
- 53 P. Mukerjee, *J. Phys. Chem.*, 1972, **76**, 565.
- 54 T. F. Hunter, *Chem. Phys. Lett.*, 1980, **75**, 152.
- 55 J. T. Edward, *J. Chem. Educ.*, 1970, **47**, 261.
- 56 A. H. Alwattar, M. D. Lumb and J. B. Birks, in *Organic Molecular Photophysics*, ed. J. B. Birks (Wiley-Interscience, New York, 1973), vol. 1, pp. 403-456.
- 57 A. L. Fischer and I. Bronstein-Bonte, *J. Photochem.*, 1985, **30**, 475.
- 58 S. L. Murov, *Handbook of Photochemistry* (M. Dekker, New York, 1973), p. 199.
- 59 G. G. Warr and F. Grieser, *Chem. Phys. Lett.*, 1985, **116**, 505.
- 60 L. B.-Å. Johansson, T. Vallmark and G. Lindblom, *J. Chem. Soc., Faraday Trans. 1*, 1985, **81**, 1389.
- 61 H. Kuhn, *J. Chem. Phys.*, 1970, **53**, 101.

Paper 6/1979; Received 8th October, 1986